ESA Climate Change Initiative – Fire_cci
O1.D2 Report on uncertainties of CC and AFL

Project Name	ECV Fire Disturbance: Fire_cci Phase 2
Contract Nº	4000115006/15/I-NB
Issue Date	07/12/2017
Version	1.1
Author	Guido van der Werf
Document Ref.	Fire_cci_O1.D2_v1.1.pdf
Document type	Internal

Project Partners

Prime Contractor/ Scientific Lead & Project Management	UAH – University of Alcala (Spain)
Earth Observation Team	UAH – University of Alcala (Spain) EHU – University of the Basque Country (Spain) UL – University of Leicester (United Kingdom) UCL – University College London (United Kingdom) ISA – School of Agriculture, University of Lisbon (Portugal)
System Engineering	BC – Brockmann Consult (Germany)
Climate Research Group	MPIC – Max Planck Institute for Chemistry (Germany) IRD - Research Institute for Development (France) LSCE - Climate and Environmental Sciences Laboratory (France) VUA - Vrije Universiteit Amsterdam (Netherlands)

Distribution

Affiliation	Name	Address	Copies
ESA	Stephen Plummer (ESA)	stephen.plummer@esa.int	electronic copy
Project Team	Emilio Chuvieco (UAH) M. Lucrecia Pettinari (UAH) Joshua Lizundia (UAH) Gonzalo Otón (UAH) Mihai Tanase (UAH) Miguel Ángel Belenguer (UAH) Aitor Bastarrika (EHU) Ekhi Roteta (EHU) Kevin Tansey (UL) Marc Padilla Parellada (UL) James Wheeler (UL) Philip Lewis (UCL) José Gómez Dans (UCL) James Brennan (UCL) Jose Miguel Pereira (ISA) Duarte Oom (ISA) Manuel Campagnolo (ISA) Thomas Storm (BC) Johannes Kaiser (MPIC) Angelika Heil (MPIC) Florent Mouillot (IRD) M. Vanesa Moreno (IRD) Philippe Ciais (LSCE) Chao Yue (LSCE) Pierre Laurent (LSCE) Guido van der Werf (VUA) Ioannis Bistinas (VUA)	emilio.chuvieco@uah.es mlucrecia.pettinari@uah.es joshua.lizundia@uah.es gonzalo.oton@uah.es mihai.tanase@uah.es miguel.belenguer@uah.es aitor.bastarrika@ehu.es ekhi.roteta@gmail.com kjt7@leicester.ac.uk mp489@leicester.ac.uk jemw3@leicester.ac.uk ucfalew@ucl.ac.uk j.gomez-dans@ucl.ac.uk james.brennan.11@ucl.ac.uk jmocpereira@gmail.com duarte.oom@gmail.com mlc@isa.ulisboa.pt thomas.storm@brockmann-consult.de j.kaiser@mpic.de a.heil@mpic.de florent.mouillot@cefe.cnrs.fr mariavanesa.morenodominguez@cefe.... philippe.ciais@lsce.ipsl.fr chaoyuejoy@gmail.com pierre.laurent@lsce.ipsl.fr guido.vander.werf@vu.nl i.bistinas@vu.nl	electronic copy

Summary

This document is the second deliverable of Option 1: Satellite-based constraints on fire fuel consumption and carbon emissions. It is part of WP120: fuel consumption from models, and it refers to the uncertainty estimations of combustion completeness and available fuel load.

	Affiliation/Function	Name	Date
Prepared	VUA	Guido van der Werf	30/11/2017
Reviewed	UAH – Project Manager	M. Lucrecia Pettinari	07/12/2017
Authorized	UAH - Science Leader	Emilio Chuvieco	07/12/2017
Accepted	ESA - Technical Officer	Stephen Plummer	07/12/2017

This document is not signed. It is provided as an electronic copy.

Document Status Sheet

Issue	Date	Details
1.0	30/09/2017	First Document Issue
1.1	07/12/2017	Addressed comments on CCI-EOPS-FIRE-MM-17-0099

Document Change Record

Issue	Date	Request	Location	Details
1.1	07/12/2017	ESA	Section 1	Clarification of method of computation of AFL and CC.
		ESA	Section 2.1	Last paragraph expanded.
		VUA	Section 2.2	Small changes in the text.
		ESA	Section 2.3.1 and 2.3.2	Text expanded.
		ESA	Figure 8	Reference to missing MERIS data not being used
		ESA	Section 3.2	Clarified reference on use of MODIS data.
		UAH	Section 6	References updated.

Table of Contents

1. Introduction 5
2. Available fuel load (AFL)..6
2.1. Introduction 6
2.2. Available information..6
2.3. Approach 7
2.3.1. Wood and foliage...7
2.3.2. Litter and cwd 7
2.3.3. Soil...8
2.4. Results 8
3. Combustion completeness (CC) 16
3.1. Introduction 16
3.2. Available information..16
3.3. Approach 16
3.4. Results 17

4. Other datasets and models 18
5. Summary, data usage, caveats 18
5.1. File contents 19
6. References 20
Annex 1: Acronyms and abbreviations 22

List of Tables

Table 1: Combustion completeness values used in GFED for various pools and minimum and maximum values used to derive upper and lower bounds in the Monte Carlo runs based on the compilation of van Leeuwen et al. (2014). Note that for deforestation regions CC values in GFED can be boosted to reflect repeated burning. 16

List of Figures

Figure 1: Fire carbon emissions (g C m^{-2} $year^{-1}$) based on Fire_cci MERIS data and the GFED modelling framework, averaged over 2005-2011. Note that tropical peatland fires as well as deforestation fires were omitted. 5

Figure 2: Live standing biomass according to the compilation of Avitabile et al. (2016) and Santoro et al. (2015) with minimum and maximum values based on 5th and 95th percentiles of higher resolution (0.01°) native grid cell values. White areas denote treeless areas. 9

Figure 3: Live standing biomass available for fire based on LIDAR measurements and a fire-induced tree mortality scalar. 10

Figure 4: Foliage AFL based on grass and leaves, the latter are converted from total leaf biomass to AFL using the fire induced tree mortality scalar. 11

Figure 5: Coarse woody debris derived from grid-cell specific tree growth and biome-specific tree turnover rates as well as a set maximum coarse woody debris turnover rate scaled down when temperature and moisture conditions inhibit heterotrophic respiration. 12

Figure 6: Surface litter derived from decaying plant litter. For most savanna fires this is the key fuel category. 13

Figure 7: Soil carbon, only available for burning when carbon densities are high as in the boreal region where the duff layer is a key fuel component. Peatlands were not included in this analysis. 14

Figure 8: Total mean AFL for the MERIS era (missing MERIS data was not accounted for), both burned-area weighted (top) and averaged over 2005-2011 (middle). The difference can be substantial (bottom). When weighted by burned area the coverage is limited to areas which had burned area over the MERIS era and these should be favoured over mean because of the temporal variability in AFL. 15

Figure 9: Combustion completeness values for the 2005-2011 period, either weighted by Fire_cci burned area (top) or averaged over the 7 year time period. The former should be preferred but only have data for areas that had burned area (the accompanying files have values for all grid cells for all months). The mean monthly values are lower than the actual values because of the temporal pattern of CC in GFED with higher values during the dry season. 17

1. Introduction

Converting new Fire_cci burned area estimates into carbon emissions requires information on fuel load and combustion completeness. This report provides gridded estimates of both parameters including an uncertainty assessment. It relies heavily on the Global Fire Emissions Database (GFED) modelling set-up (van der Werf et al., 2017) and the field measurement database of van Leeuwen et al. (2014). The resulting gridded datasets mainly serve to facilitate WP130, "Synergistic carbon flux calculation" for option 1 of the European Space Agency (ESA) funded Fire_cci project.

This report is structured to first introduce the key parameters for available fuel load (AFL) and combustion completeness (CC), followed by a description of how the uncertainty range of both parameters was calculated. The key objective is to lay the foundation for estimating new fire carbon emissions estimates from the Fire_cci project (as shown for example in Figure 1 where the existing GFED modelling framework was ran using Fire-cci MERIS data instead of GFED burned area) and provide boundary conditions to evaluate efforts to combine fire radiative energy (FRE) and burned area approaches to estimate fuel consumption (Andela et al., 2016). Uncertainty estimates are much needed and a notoriously difficult subject in fire emissions research because few parameters required to calculate emissions come with reliable uncertainty estimates. All estimates presented here are in units of g C m^{-2} and on a 0.25° grid. If input data was reported in dry matter units a carbon content of 50% was assumed to convert to carbon units.

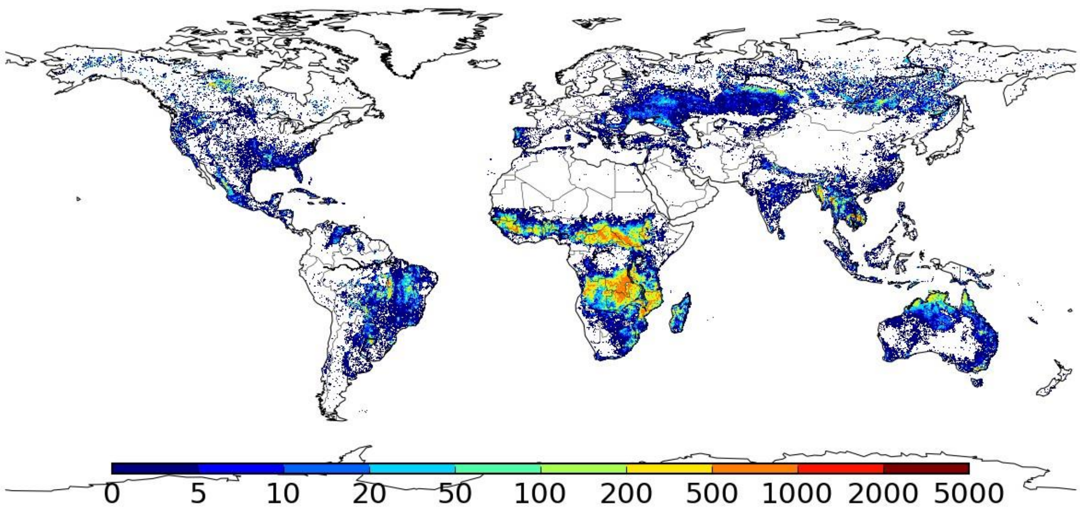

Figure 1: Fire carbon emissions (g C m^{-2} $year^{-1}$) based on Fire_cci MERIS data and the GFED modelling framework, averaged over 2005-2011. Note that tropical peatland fires as well as deforestation fires were omitted.

AFL and CC on one hand and its uncertainty on the other hand are derived from two somewhat different approaches. The monthly "best" values for both were based on actual AFL and CC values for the Fire CCI MERIS burned area time period (2005-2011). On a biome level, these estimates have been calibrated with measurements but the spatial match between modelled and measured values is still only reasonable at best (van der Werf et al., 2017). The uncertainty (minimum and maximum values based on 2σ uncertainty) is based on a Monte Carlo simulation with 1000 runs. This was not done for the 2005-2011 period but the model was first span up to equilibrium using the same datasets as for the "best" values, and after that we ran 1000 runs of 100 years each with varying parameters until that had reached equilibrium. It is thus based on the average burned area and other input datasets instead of actual 2005-2011 data which would require much more computing power while not influencing results substantially. For those grid cells that have seen dramatic land use or land cover change in recent years the two approaches may diverge more.

2. Available fuel load (AFL)

2.1. Introduction

Fuel load can be broadly categorized in live biomass, surface litter, and soil carbon. The amount of carbon in each category and the availability for fires varies widely between biomes. In general forests have most live biomass but whether that is available for combustion depends on the type of forest; in boreal forests only a small fraction of the stems is consumed, especially in the case of ground fires, while in tropical deforestation fires all carbon can be consumed if the biomass is burned repetitively. The difference between total live biomass and available biomass is represented by the fire-induced mortality scalar which converts fuel load into available fuel load. The amount of carbon in this category depends on tree density, tree type, and tree productivity. The live biomass will be categorized in wood (stems) and leaves, the latter including grass.

Surface litter is virtually always available for fire so there is no distinction between total surface litter and available surface litter. This category is probably the most important biomass category for fires. In forests, part of the surface litter is relatively coarse, while in grasslands fine litter dominates. Total carbon available in this category depends mostly on vegetation productivity and turnover rates, and is also impacted by fuelwood collection and herbivory. In general, both productivity and turnover rates are higher in the tropics than in temperate and boreal ecosystems so the gradient in AFL is not as obvious as for live biomass because while carbon gains in extratropical regions are lower than in the tropics, its breakdown is slow as well. A special fuel category is the duff layer, found in boreal ecosystems with slow turnover rates. It consists of highly decomposed plant material and may be tens of centimetres thick on top of the organic soil, with the top layer still recognizable as plant material. The thickness of this layer, the key fuel source in boreal ecosystems, depends mostly on soil type and tree species. Surface litter will be reported as fine or coarse litter, the latter will be referred to as coarse woody debris (cwd).

The last category is soil carbon. It includes the lowest layers of the duff layer, belowground wood, and carbon-rich peatlands. These occur worldwide but are most concentrated in the boreal and tropical forest regions where slow drainage prevents decomposition. This study excludes tropical peatland as a fuel source, even though it is the main fuel source in Indonesia. Over the next year at least two LIDAR based studies will be published that may lead to better estimates of both fuel consumption and its uncertainty.

2.2. Available information

The only fuel category that can be (indirectly) observed from space is live aboveground biomass, with vegetation indices such as the normalized difference vegetation index (NDVI) or the fraction of absorbed photosynthetically active radiation (fAPAR) being related to photosynthesizing parts of the live biomass and light detection and ranging (LIDAR) instruments often used to estimate vegetation height, which can then be translated to biomass using height to biomass conversions. In GFED, fAPAR is used to derive net primary production (NPP) in a light use efficiency model. Fractional tree cover maps govern the allocation to grasses and leaves and total carbon content of those pools depends on the input from NPP and losses through decay, grazing, and fires.

The LIDAR measurements used most frequently on pan-tropical or global studies are from measurements of the Geoscience Laser Altimeter System (GLAS), onboard the Ice, Cloud, and land Elevation Satellite (ICESat). These are the basis for estimating live standing biomass and within the GlobBiomass (http://globbiomass.org, accessed November 2017) project efforts have been made to merge existing, but sometimes contradictory, datasets.

For surface litter and soil carbon the situation is much worse because these are not observable from space and mostly derived from modelling or based on lookup tables and detailed vegetation and topography maps. For North America the situation is improving due to extensive fieldwork covering more than 1000 plots but those results were not available at the time of writing.

2.3. Approach

2.3.1. Wood and foliage

For live standing biomass we have used the GEOCARBON merged biomass dataset (downloaded from https://www.bgc-jena.mpg.de on April 25, 2017). The IceSAT GLAS measurements were made in 2007 and 2008 and both Baccini et al. (2012) and Saatchi et al. (2011) constructed biomass datasets for the tropics based on these estimates. Avitabile et al. (2016) then combined both datasets with a reference dataset to provide the map we used here as a best estimate where extra-tropical values were based on Santoro et al. (2015). For the tropics, Herold et al. (2016) has merged both datasets. Conversion of LIDAR derived height to biomass is based on allometric models which are, in general, based on average wood densities. In regions where wood density varies uncertainties may be large. While uncertainties reported in both Baccini et al. (2012) and Saatchi et al. (2011) were relatively small (less than 10% for coarse grid cells), the compilation of Saatchi et al. (2011) indicated that this may have been an underestimate and we therefore doubled it to 20% uncertainty (1σ) in the Monte Carlo simulation. The resulting uncertainties will be reported as 2σ.

The amount of foliage was derived from GFED. Of all modelling approaches for fire, that framework has been compared to field data most extensively. Uncertainties were based on a Monte Carlo approach (1000 runs) where we used 1σ values of 25% for the light use efficiency scalar, pool turnover rates, herbivore consumption, and livestock foliage requirements.

2.3.2. Litter and cwd

Surface litter is derived from decaying live biomass. Because there are no satellite observations of the amount of surface litter it is usually derived from modelling. For most biomes this is the key source of fuel. Here we report the GFED estimates that have been compared to field studies and derive uncertainties just like those of live foliage from a Monte Carlo simulation as described above, but increased the uncertainty of the coarse woody debris pool to 35% to cover the wide range of turnover rates reported in the literature. Uncertainty of all other pools, including the key ones for deriving fine surface litter, were set at 25% but are in reality larger because also the light use efficiency scalar was variable in the Monte Carlo simulation and this feeds via NPP directly to the carbon pools. These percentages (35 and 25%) are somewhat arbitrary but based loosely on the Van Leeuwen et al. (2014) compilation to reflect the range of measurements, which is highest for coarse woody debris. Since coarse woody debris decays into other pools it will boost the actual uncertainty in the simulation of those pools which become then more similar in actual uncertainty.

2.3.3. Soil

Just like surface litter, soil carbon cannot be measured from space. All the assigned uncertainties in the Monte Carlo simulation trickle down to the amount of soil carbon and that is also the estimates shown here. However, the actual uncertainty may be larger because there are very limited observations to compare the derived range to.

2.4. Results

In the next pages maps of the various fuel categories are shown, starting with the LIDAR based total standing biomass followed by the fraction that is available for burning. The difference is based on the fire induced mortality rate. Maps are shown for the most likely estimates (either LIDAR based or GFED standard run), and the minimum and maximum values based on the GFED Monte Carlo simulation. The values are based on the 2.5th and 97.5th percentile, corresponding to -2 and +2σ. So while parameter uncertainty was reported as 1σ values, the minimum and maximum are based on 2σ.

In general the spatial patterns of most fuel categories are relatively similar with highest values in tropical forests followed by other forest types, woodlands, savannas, and grasslands. But this gradient becomes less obvious further down the carbon chain from carbon uptake to respiration. For example, coarse woody debris in many extratropical forest areas exceeds tropical forest values despite much lower tree density due to lower turnover rates. For soil carbon the patterns are even opposite with boreal forests having high AFL there while it is non-existent in most tropical regions.

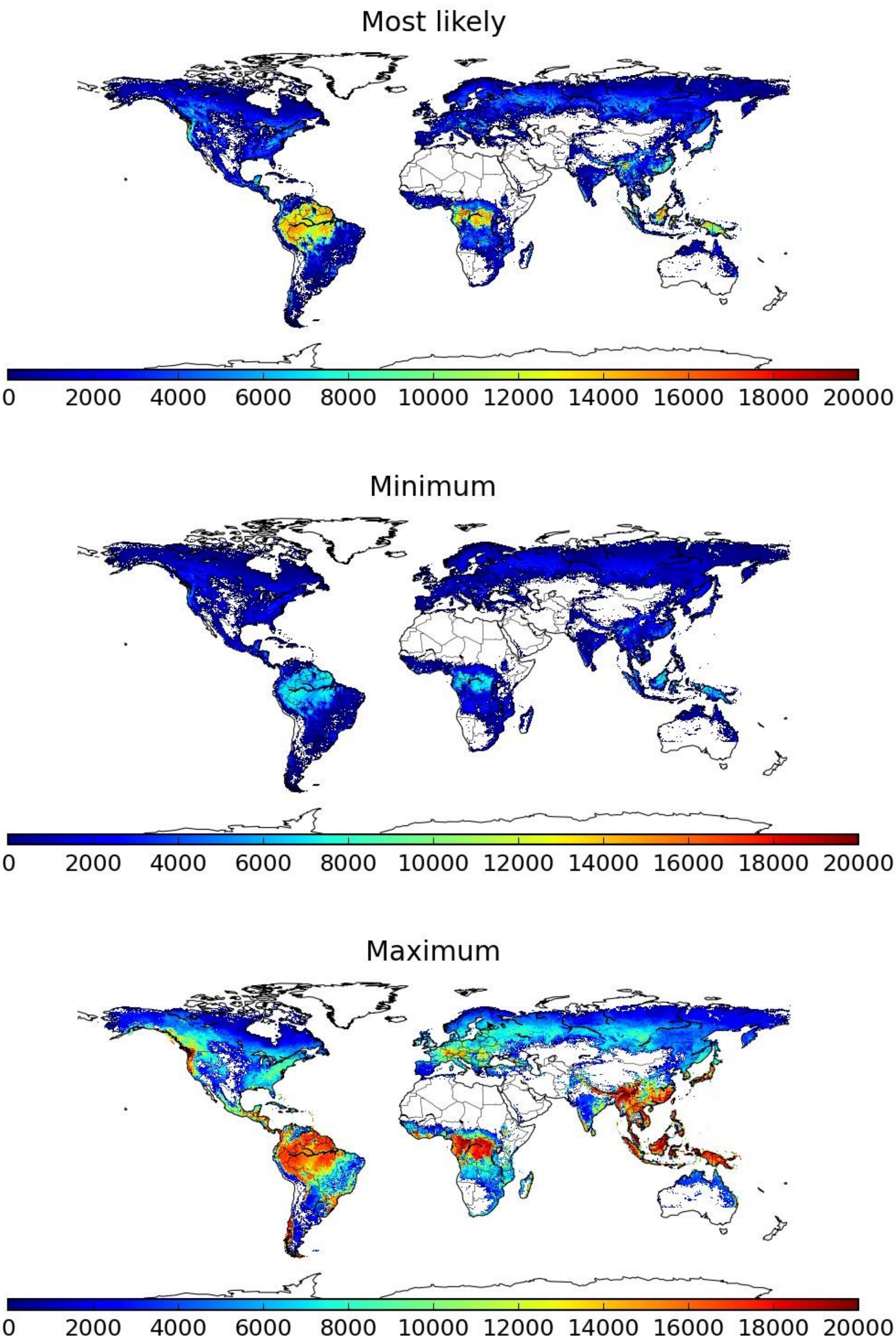

Figure 2: Live standing biomass according to the compilation of Avitabile et al. (2016) and Santoro et al. (2015) with minimum and maximum values based on 5th and 95th percentiles of higher resolution (0.01°) native grid cell values. White areas denote treeless areas.

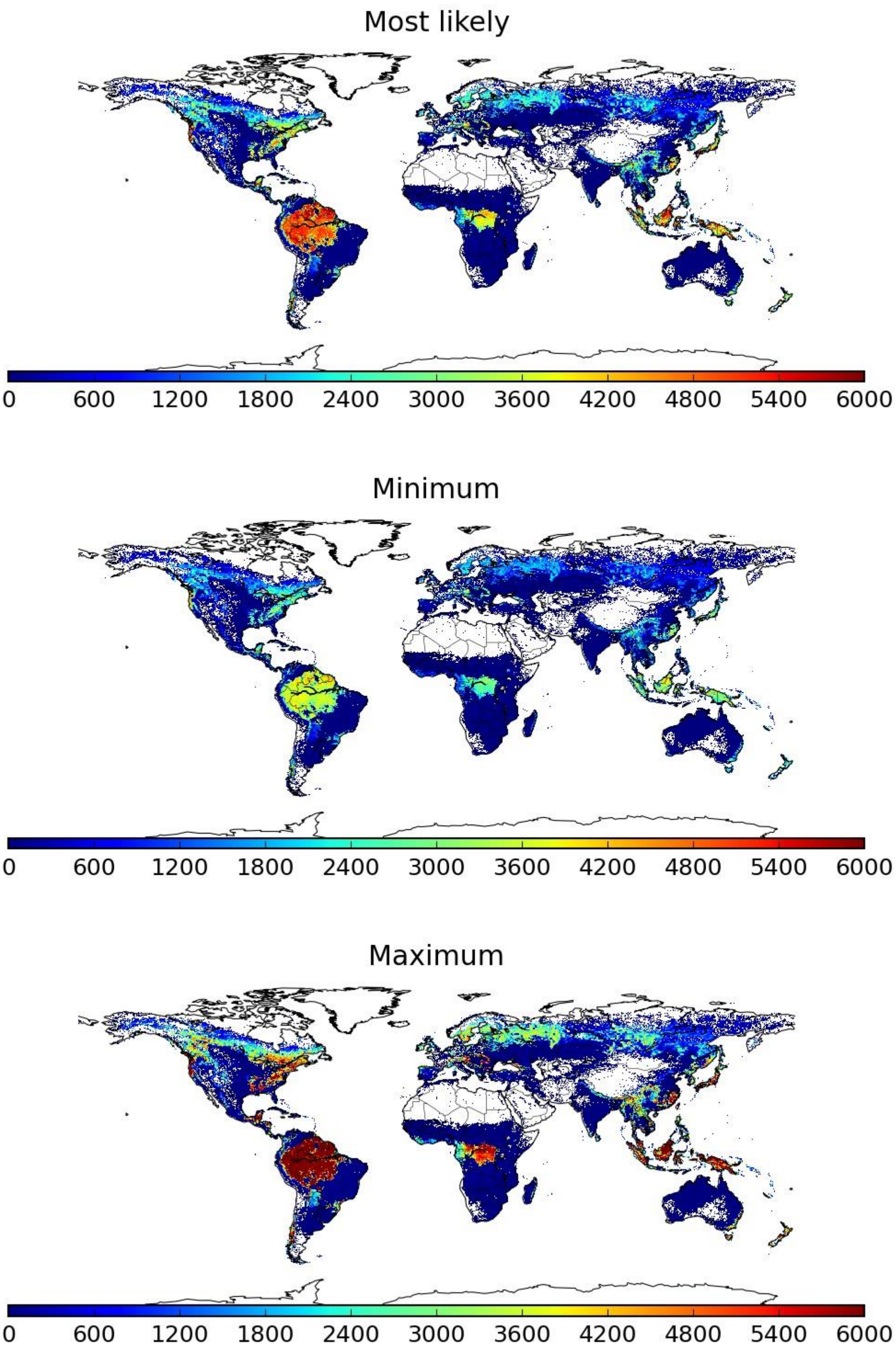

Figure 3: Live standing biomass available for fire based on LIDAR measurements and a fire-induced tree mortality scalar.

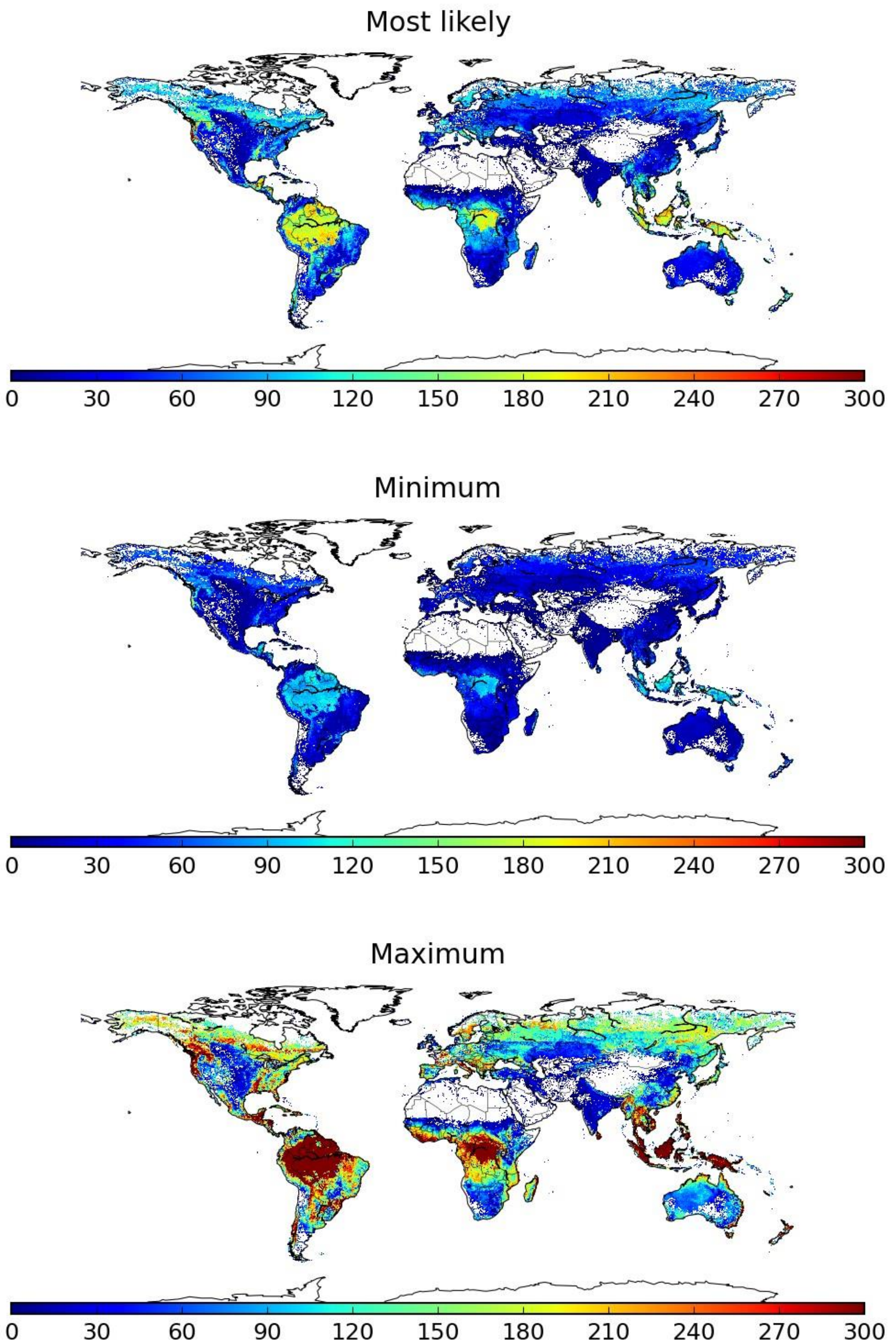

Figure 4: Foliage AFL based on grass and leaves, the latter are converted from total leaf biomass to AFL using the fire induced tree mortality scalar.

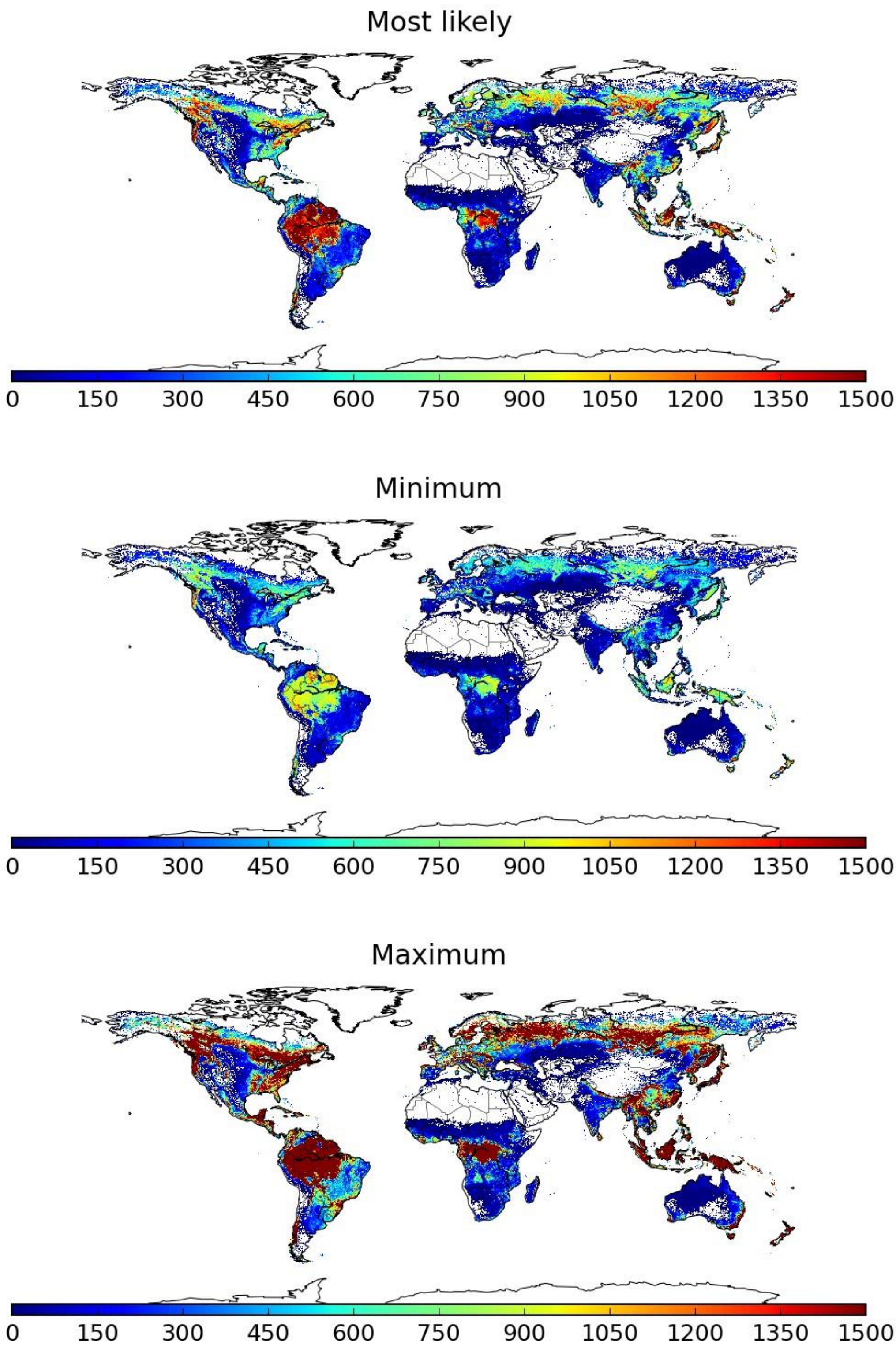

Figure 5: Coarse woody debris derived from grid-cell specific tree growth and biome-specific tree turnover rates as well as a set maximum coarse woody debris turnover rate scaled down when temperature and moisture conditions inhibit heterotrophic respiration.

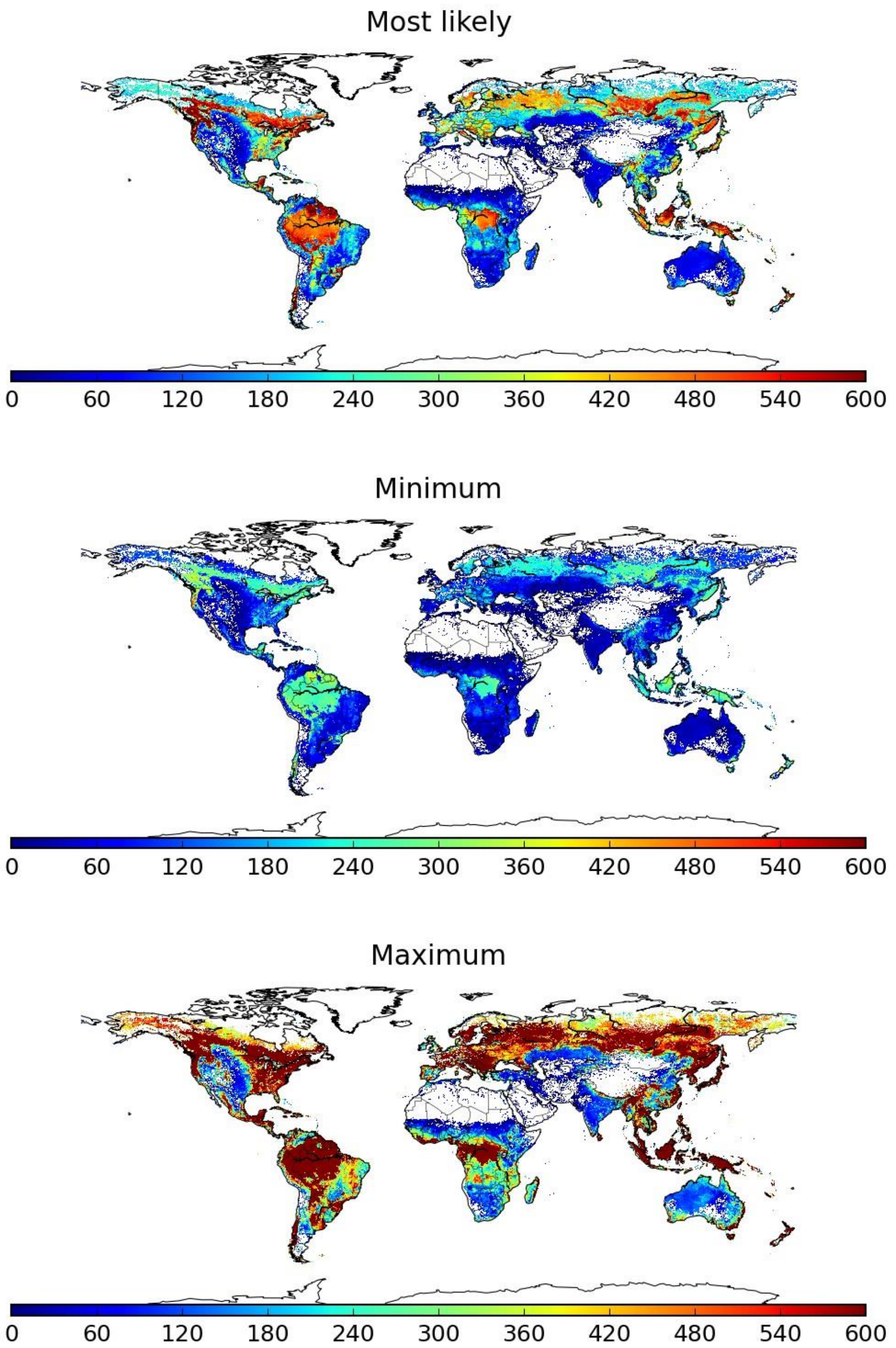

Figure 6: Surface litter derived from decaying plant litter. For most savanna fires this is the key fuel category.

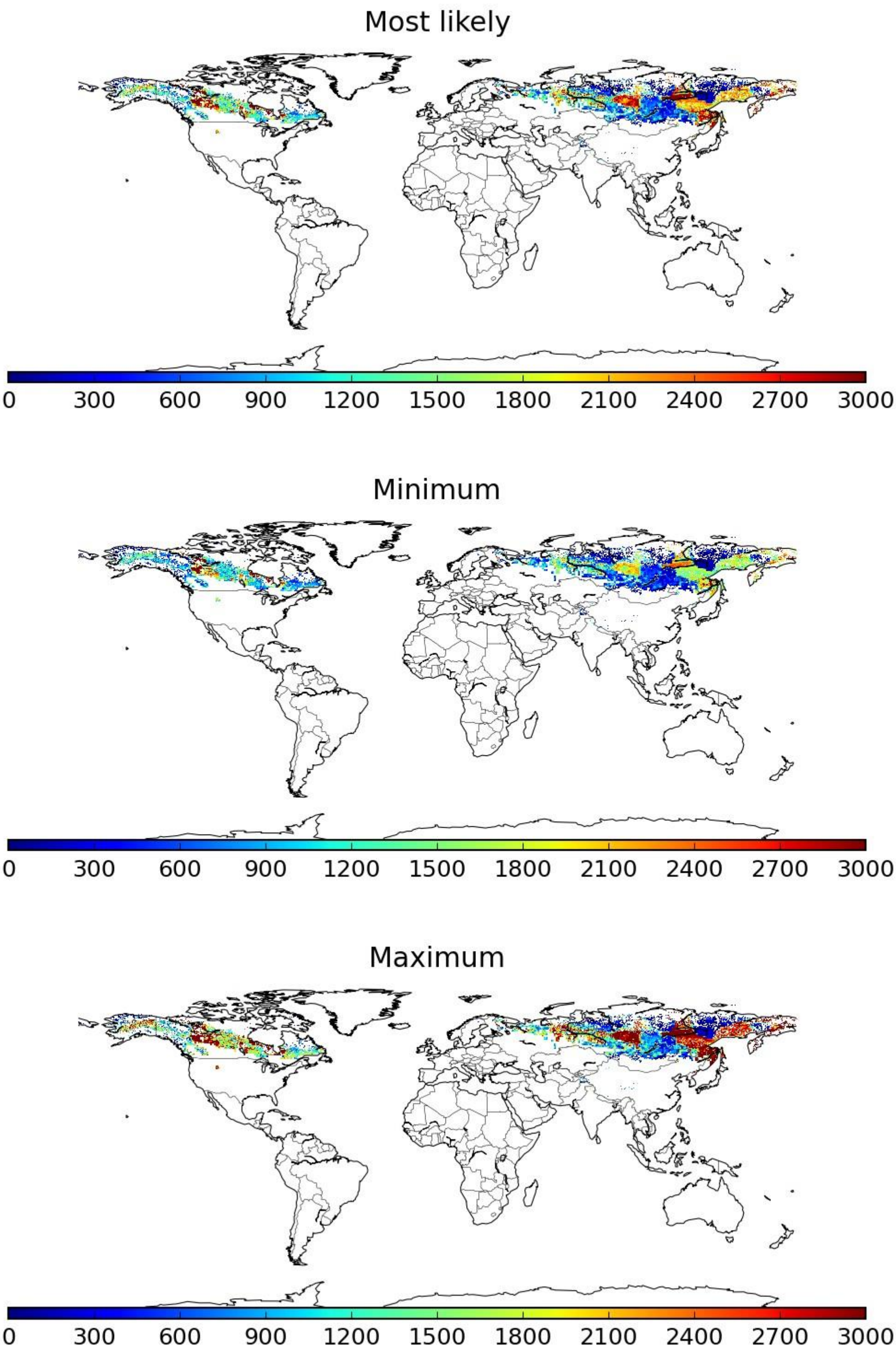

Figure 7: Soil carbon, only available for burning when carbon densities are high as in the boreal region where the duff layer is a key fuel component. Peatlands were not included in this analysis.

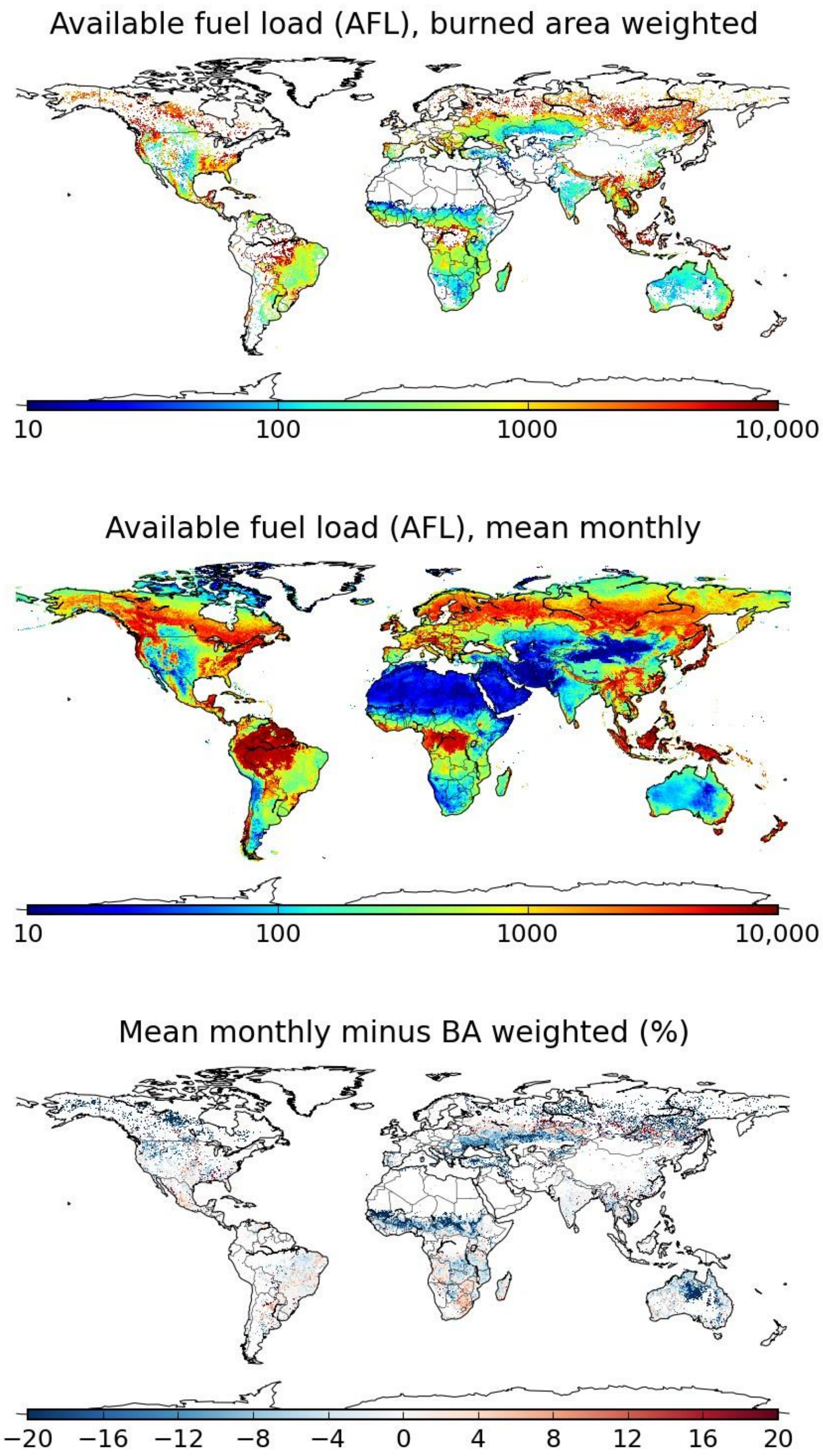

Figure 8: Total mean AFL for the MERIS era (missing MERIS data was not accounted for), both burned-area weighted (top) and averaged over 2005-2011 (middle). The difference can be substantial (bottom). When weighted by burned area the coverage is limited to areas which had burned area over the MERIS era and these should be favoured over mean because of the temporal variability in AFL.

3. Combustion completeness (CC)

3.1. Introduction

The fraction of the available fuel or biomass that is actually combusted is called combustion completeness. In the past the term combustion factor was also used for this but has become obsolete to avoid confusion with emission factors, used to convert dry matter or carbon emissions to those of trace gases and aerosols. Combustion completeness is in general inversely related to fuel surface to area ratio as well as to density, with fine fuels often combusting completely while larger diameter fuels often remain after a fire.

3.2. Available information

Sá et al. (2007) showed that satellite data can be used to inform about combustion completeness and more recently other researchers have furthered this approach using native resolution MODIS data (Lewis et al. (2009) and subsequent work not published yet). Rogers et al. (2015) have used spectral indices to better contrast the different fire regimes in the boreal region, parameterizing both fire-induced mortality rates and combustion completeness. While these approaches may lead to more refined spatial patterns of combustion completeness, it is usually based on relating measurements on the ground to spectral indices and to date no consistent global dataset exists that can cover multiple biomes (Veraverbeke and Hook, 2013). Probably the most reliable estimates are therefore derived from ground studies, for example those found in the compilation of van Leeuwen et al. (2014).

3.3. Approach

We extracted burned area weighted GFED CC values for the various fuel categories and expanded the range of minimum and maximum values used in that approach to reflect the full range measured in field studies (Table 1).

Table 1: Combustion completeness values used in GFED for various pools and minimum and maximum values used to derive upper and lower bounds in the Monte Carlo runs based on the compilation of van Leeuwen et al. (2014). Note that for deforestation regions CC values in GFED can be boosted to reflect repeated burning.

Fuel category	GFED		Monte Carlo	
	Minimum	Maximum	Minimum	Maximum
Leaves	80%	100%	56%	100%
Fine litter	90%	100%	60%	100%
Coarse litter	30%	60%	4%	60%
Wood	20%	40%	4%	55%

3.4. Results

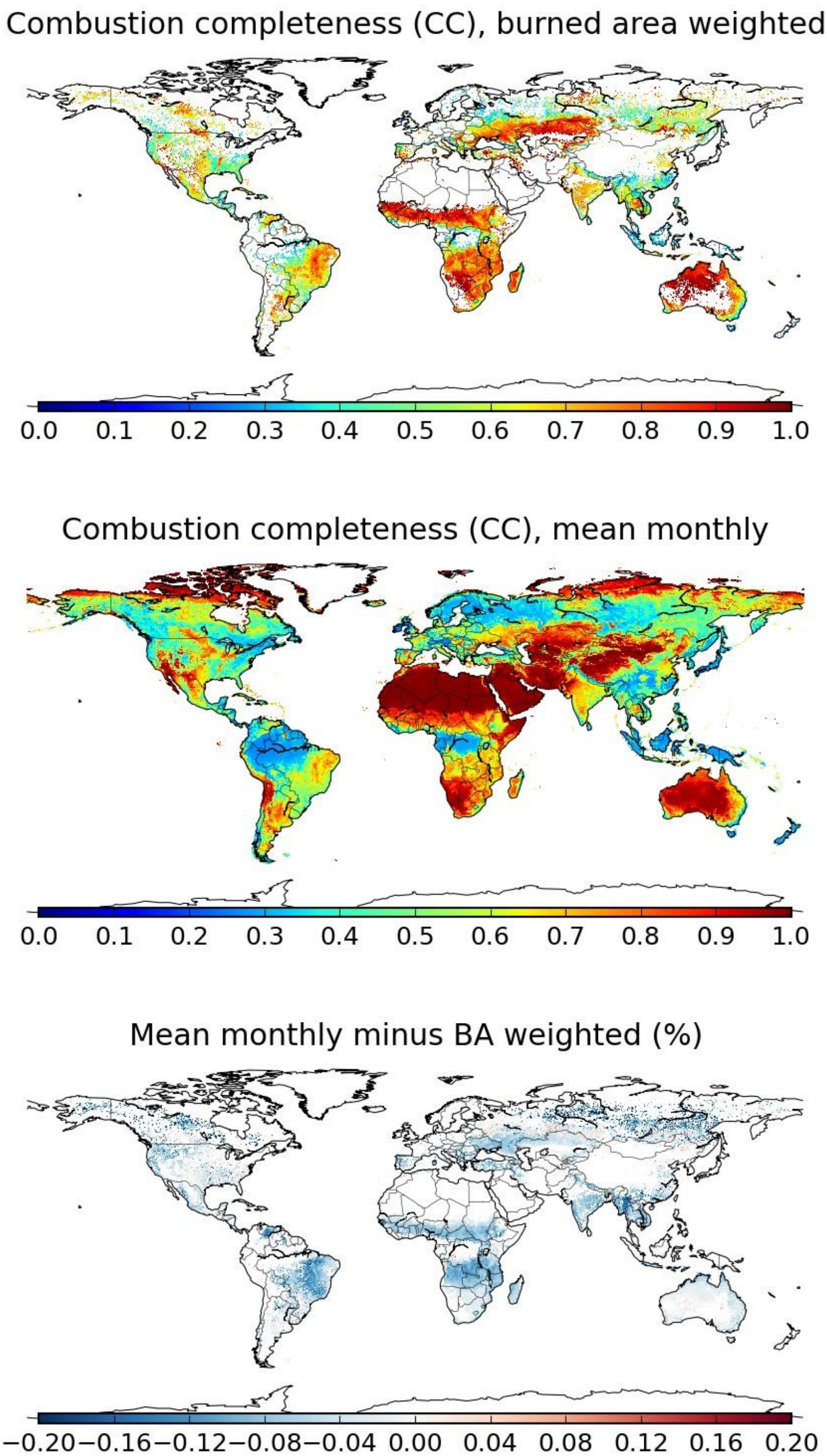

Figure 9: Combustion completeness values for the 2005-2011 period, either weighted by Fire_cci burned area (top) or averaged over the 7 year time period. The former should be preferred but only have data for areas that had burned area (the accompanying files have values for all grid cells for all months). The mean monthly values are lower than the actual values because of the temporal pattern of CC in GFED with higher values during the dry season.

4. Other datasets and models

As outlined in the original proposal for Option 1, the focus of WP120 of that proposal was on the GFED-GFED modelling framework but we aimed to use additional models from the FireMIP exercise (Hantson et al., 2016; Rabin et al., 2017). In this report we refrained from using AFL and CC from those dynamic models because they have in general a high bias in herbaceous ecosystems and a low bias in woody ecosystems. The reported uncertainty would therefore be substantially higher than it actually is (Stéphane Mangeon, personal communication, manuscript in preparation).

During the time frame of Option 1 the fuel consumption database will be updated when possible (no new published papers in the past year but both ABOVE and several US campaigns will offer new data in the next year).

5. Summary, data usage, caveats

In this report we have calculated best estimates, minimum values, and maximum values for aboveground fuel load (AFL) and combustion completeness (CC). These estimates are mostly derived from the GFED modelling framework, LIDAR-based vegetation density estimates, and ground measurements. In combination with burned area these layers can be used to calculate fire carbon emissions. In addition, they may provide guidance of the fidelity of total fuel consumption estimates derived from FRE-based emissions divided by burned area (Andela et al., 2016).

Total fuel consumption (FC) can be derived following:

$$FC = \sum_{i=1}^{i=4} FL_i \times CC_i \times mortality_i$$

where i denotes the fuel category (leaves, wood, fine litter, coarse litter). Fire induced mortality rates only apply to the wood and leaf category and is unity for the other categories, multiplying total fuel load (FL) with that scalar yields available fuel load.

All data presented here is based on burned area weighted values. However, both AFL and CC vary not only spatially but also temporally. For example, early season savanna fires still burn grasses while these have all gone dormant later in the season. In addition, the AFL and CC values are somewhat dependent on burned area and thus the spin-up in the model. If burned area datasets therefore change (for example due to a boost from adding Sentinel-2 small fire burned area), it is advisable to recalibrate the AFL and CC fields. This can be done relatively easily because GFED has already been modified to run Fire_cci burned area data for most fire types. The exception are deforestation fires where active fire persistence is a key input dataset and tropical peat fires where the 0.25° burned area should be categorized into peat or non-peat burning. To provide some temporal variability, total AFL and CC values are also given for the Fire_cci 2005-2011 period with a monthly resolution.

Since AFL and CC variations over time are best weighted by burned area, no values are given here for grid cells without fire. This concerns mostly ice and deserts but also areas that may burn in the future such as tundra. The AFL and CC values for 2005-2011 can be used to compute emissions for those grid cells, but if uncertainty estimates are required these can be based on the Monte Carlo runs that will be archived for the duration of the CCI project.

Deforestation and tropical peatland fires are not included in the AFL and CC values presented here. These require additional information on fire persistence and the partitioning of burned area in different fire types, which will be done during WP130.

5.1. File contents

The data is archived as an HDF5 file and will be transferred to the MPIC server in a format consistent with other datasets. The file structure is as follows, with

<YEAR> denoting the years 2005-2011, and <MONTH> used to identify the various months with January being 01, February 02, etc. Note that CC of soil carbon is unity:

```
/annual/
       /<YEAR>/
              /<MONTH>/
                      /AF
                       L
                     /CC
/min/
     /foliage
     /wood
     /litter
     /coarse_litter
     /soil
/median/
     /foliage
     /wood
     /litter
     /coarse_litter
     /soil
/max/
     /foliage
     /wood
     /litter
     /coarse_litter
     /soil
```

6. References

Andela, N., van der Werf, G. R., Kaiser, J., van Leeuwen, T. T., Wooster, M. J. and Lehmann, C. E. R.: Biomass burning fuel consumption dynamics in the tropics and subtropics assessed from satellite, Biogeosciences, 13(12), 3717–3734, doi:10.5194/bg-13-3717-2016, 2016.

Avitabile, V., Herold, M., Heuvelink, G. B. M., Lewis, S. L., Phillips, O. L., Asner, G. P., Armston, J., Ashton, P. S., Banin, L., Bayol, N., Berry, N. J., Boeckx, P., de Jong, B. H. J., DeVries, B., Girardin, C. A. J., Kearsley, E., Lindsell, J. A., Lopez-Gonzalez, G., Lucas, R., Malhi, Y., Morel, A., Mitchard, E. T. A., Nagy, L., Qie, L., Quinones, M. J., Ryan, C. M., Ferry, S. J. W., Sunderland, T., Laurin, G. V., Gatti, R. C., Valentini, R., Verbeeck, H., Wijaya, A. and Willcock, S.: An integrated pan-tropical biomass map using multiple reference datasets, Global Change Biology, 22(4), 1406–1420, doi:10.1111/gcb.13139, 2016.

Baccini, A., Goetz, S. J., Walker, W. S., Laporte, N. T., Sun, M., Sulla-Menashe, D., Hackler, J., Beck, P. S. A., Dubayah, R., Friedl, M. A., Samanta, S. and Houghton, R. A.: Estimated carbon dioxide emissions from tropical deforestation improved by carbon-density maps, Nature Climate Change, 2(3), 182–185, doi:10.1038/NCLIMATE1354, 2012.

Hantson, S., Arneth, A., Harrison, S. P., Kelley, D. I., Prentice, I. C., Rabin, S. S., Archibald, S., Mouillot, F., Arnold, S. R., Artaxo, P., Bachelet, D., Ciais, P., Forrest, M., Friedlingstein, P., Hickler, T., Kaplan, J. O., Kloster, S., Knorr, W., Lasslop, G., Li, F., Mangeon, S., Melton, J. R., Meyn, A., Sitch, S., Spessa, A., van der Werf, G. R., Voulgarakis, A. and Yue, C.: The status and challenge of global fire modelling, Biogeosciences, 13(11), 3359–3375, doi:10.5194/bg-13-3359-2016, 2016.

Herold M., Heuvelink G., Lewis S.L., Phillips O.L., Asner G. P. et al. An integrated pan-tropical biomass map using multiple reference datasets. Global Change Biology, 2016, doi:10.1111/gcb.13139, 2016

Lewis, P., Quaife, T, Gomez-Dans, J., Disney, M, Wooster, M, Roy, D., Pinty, B.. Modelling the impact of wildfire on spectral reflectance. International Geoscience and Remote Sensing Symposium (IGARSS). 4. IV-1019 . 10.1109/IGARSS.2009.5417553, 2009

Rabin, S. S., Melton, J. R., Lasslop, G., Bachelet, D., Forrest, M., Hantson, S., Kaplan, J. O., Li, F., Mangeon, S., Ward, D. S., Yue, C., Arora, V. K., Hickler, T., Kloster, S., Knorr, W., Nieradzik, L., Spessa, A., Folberth, G. A., Sheehan, T., Voulgarakis, A., Kelley, D. I., Prentice, I. C., Sitch, S., Harrison, S. and Arneth, A.: The Fire Modeling Intercomparison Project (FireMIP), phase 1: experimental and analytical protocols with detailed model descriptions, Geoscientific Model Development, 10(3), 1175–1197, doi:10.5194/gmd-10-1175-2017, 2017.

Rogers, B. M., Soja, A. J., Goulden, M. L. and Randerson, J. T.: Influence of tree species on continental differences in boreal fires and climate feedbacks, Nature Geoscience, 8(3), 228–234, doi:10.1038/NGEO2352, 2015.

Saatchi, S. S., Harris, N. L., Brown, S., Lefsky, M., Mitchard, E. T. A., Salas, W., Zutta, B. R., Buermann, W., Lewis, S. L., Hagen, S., Petrova, S., White, L., Silman, M. and Morel, A.: Benchmark map of forest carbon stocks in tropical regions across three continents, PNAS, 108(24), 9899–9904, doi:10.1073/pnas.1019576108, 2011.

Santoro, M., Beaudoin, A., Beer, C., Cartus, O., Fransson, J. B. S., Hall, R. J., Pathe, C., Schmullius, C., Schepaschenko, D., Shvidenko, A., Thurner, M. and Wegmueller, U.: Forest growing stock volume of the northern hemisphere: Spatially explicit estimates for 2010 derived from Envisat ASAR, Remote Sensing of Environment,168, 316–334, doi:10.1016/j.rse.2015.07.005, 2015.

Sá, A. C. L., Pereira, J. M. C. and Silva, J. M. N.: Estimation of combustion completeness based on fire-induced spectral reflectance changes in a dambo grassland (Western Province, Zambia), International Journal of Remote Sensing, 26(19), 4185–4195, doi:10.1080/01431160500113468, 2007.

van der Werf, G. R., Randerson, J. T., Giglio, L., van Leeuwen, T. T., Chen, Y., Rogers, B. M., Mu, M., van Marle, M. J. E., Morton, D. C., Collatz, G. J., Yokelson, R. J. and Kasibhatla, P. S.: Global fire emissions estimates during 1997-2015, Earth Syst. Sci. Data Discuss., 1–43, doi:10.5194/essd-2016-62, 2017.

van Leeuwen, T. T., van der Werf, G. R., Hoffmann, A. A., Detmers, R. G., Ruecker, G., French, N. H. F., Archibald, S., Carvalho, J. A. J., Cook, G. D., de Groot, W. J., Hely, C., Kasischke, E. S., Kloster, S., McCarty, J. L., Pettinari, M. L., Savadogo, P., Alvarado, E. C., Boschetti, L., Manuri, S., Meyer, C. P., Siegert, F., Trollope, L. A. and Trollope, W. S. W.: Biomass burning fuel consumption rates: a field measurement database, Biogeosciences, 11(24), 7305–7329, doi:10.5194/bg-11-7305-2014, 2014.

Veraverbeke, S. and Hook, S. J.: Evaluating spectral indices and spectral mixture analysis for assessing fire severity, combustion completeness and carbon emissions, Int. J. Wildland Fire, 22(5), 707–14, doi:10.1071/WF12168, 2013.

Annex 1: Acronyms and abbreviations

AFL	Available fuel load
CC	Combustion completeness
CCI	Climate Change Initiative
Cwd	Coarse woody debris
ESA	European Space Agency
ECV	Essential Climate Variables
fAPAR	Fraction of Absorbed Photosynthetically Active Radiation
FC	Fuel consumption
FireMIP	Fire Modelling Intercomparison Project
FL	Fuel load
FRE	Fire radiative energy
GFED	Global Fire Emissions Database
GLAS	Geoscience Laser Altimeter System
ICESat	Ice, Cloud and land Elevation Satellite
LIDAR	Light detection and ranging
MERIS	Medium Resolution Imaging Spectrometer
MODIS	Moderate Resolution Imaging Spectroradiometer
MPIC	Max Planck Institute for Chemistry
NDVI	Normalized Difference Vegetation Index
NPP	Net primary production